Research Article | Vol. 29, No. 3 / 1 February 2021 / Optics Express 3055
Optics EXPRESS

Finite-difference time-domain analyses of active cloaking for electrically-large objects

TOMASZ P. STEFAŃSKI,[1,3] KONSTANTINOS BASKOURELOS,[2] AND KOSMAS L. TSAKMAKIDIS[2,4]

[1] *Faculty of Electronics, Telecommunications, and Informatics, Gdansk University of Technology, 80-233 Gdansk, Poland*
[2] *Section of Condensed Matter Physics, Department of Physics, National and Kapodistrian University of Athens, Panepistimioupolis, GR-157 84 Athens, Greece*
[3] *tomasz.stefanski@pg.edu.pl*
[4] *ktsakmakidis@phys.uoa.gr*

Abstract: Invisibility cloaking devices constitute a unique and potentially disruptive technology, but only if they can work over broad bandwidths for electrically-large objects. So far, the only known scheme that allows for broadband scattering cancellation from an electrically-large object is based on an active implementation where electric and magnetic sources are deployed over a surface surrounding the object, but whose 'switching on' and other characteristics need to be known (determined) *a priori*, before the incident wave hits the surface. However, until now, the performance (and potentially surprising) characteristics of these devices have not been thoroughly analysed computationally, ideally directly in the time domain, owing mainly to numerical accuracy issues and the computational overhead associated with simulations of electrically-large objects. Here, on the basis of a finite-difference time-domain (FDTD) method that is combined with a perfect (for FDTD's discretized space) implementation of the total-field/scattered-field (TFSF) interface, we present detailed, time- and frequency-domain analyses of the performance and characteristics of active cloaking devices. The proposed technique guarantees the isolation between scattered- and total-field regions at the numerical noise level (around −300 dB), thereby also allowing for accurate evaluations of the scattering levels from imperfect (non-ideal) active cloaks. Our results reveal several key features, not pointed out previously, such as the suppression of scattering at certain frequencies even for imperfect (time-delayed) sources on the surface of the active cloak, the broadband suppression of back-scattering even for imperfect sources and insufficiently long predetermination times, but also the sensitivity of the scheme on the accurate switching on of the active sources and on the predetermination times if broadband scattering suppression from all angles is required for the electrically-large object.

1. Introduction

Electromagnetic cloaking represents an exciting emerging technology, unattainable with ordinary materials, requiring the use of man-made engineered media, known as metamaterials. In principle, such a technology, if it could be made broadband and for electrically-large objects (much larger than the wavelength of the incident wave), is better than well-known 'stealth' or camouflage technologies [1] as it does not just make an object 'black' (absence of back-scattering) or impossible to detect owing, e.g., to induced multiple-angle scattering, but it, effectively, reduces the scattering cross-section of an object to that of a single point (zero) - thereby making the object completely undetectable, even interferometrically.

For perfect invisibility, the wave incident on the cloaked object should be everywhere (outside the cloak) exactly the same as it would have been if the cloaked region had been free space. In other words, there should not be any scattered field in the area outside the cloaked region. A linear, non-magnetized, passive cloak whose material parameters do not change with time

#413043 https://doi.org/10.1364/OE.413043
Journal © 2021 Received 21 Oct 2020; revised 14 Dec 2020; accepted 14 Dec 2020; published 19 Jan 2021

Optics EXPRESS

cannot, as it currently appears to be the case, provide perfect invisibility of electrically-large objects to wideband incident waves [2]. In general, there are two approaches allowing for the reduction of the scattering cross-section (SCS) of an object, namely (i) using active sources and the surface equivalence theorem, (ii) applying metamaterial, plasmonic or other judicious coatings. In the former approach (i), a broadband perfect SCS reduction is possible, but the characteristics of the incident wave need to be known *a priori* [3]. In the latter approach (ii), a shell of metamaterial can achieve cloaking of an electrically-large object for narrowband (near-monochromatic) electromagnetic waves [2]. For a review of various cloaking techniques, one may refer to Refs. [4,5]. However, all approaches to electromagnetic cloaking do require full-wave computational corroborations and elaborations that allow for additional insights and the quantitative analysis of realistic effects. It is the objective of the present work to present and deploy such a highly accurate (and specifically suitable for the present problem, as explained below) formulation of the full-wave finite-difference time-domain (FDTD) method of analysis [6], aiming at analysing the performance of active ('predetermined') invisibility cloaks for electrically-large objects.

The aforementioned interesting approach-(i) to cloaking (i.e., active sources and the surface equivalence theorem) has been introduced and studied quasi-analytically in [3]. Incident waves are measured near the surface of the cloaking volume, and appropriate surface sources excite the domain with analytically calculated waveforms. For a perfect (ideal) implementation, each source waveform depends on measurements in all sensing points in present and past times. A distinction was therefore made between true-cloaking and approximate quasi-cloaking schemes. The former approach employs surface sources whose values are calculated from the wave measurements in present and past times in all the sensing points near the cloaking volume. In such a case, a pulse of the incident wave remains unchanged while propagating through the cloak. The latter approach uses surface sources whose waveforms are obtained from local measurements only. Distortions of a transmitted pulse through such a cloak may then be observed. Overall, it can be concluded that perfect and broadband SCS reduction of electrically-large objects can be achieved in the limiting case of 'predetermined' cloaking, i.e., when the parameters of an incident wave are known *a priori*. Owing to the essentially analytical nature of that analysis, precise measurements of the wave scattering when imperfect cloaking is applied were not reported.

The same approach to the cloaking problem has also been studied in [7]. A predetermined cloaking allowing for the cancellation of electromagnetic scattering by using an array of sources was simulated using commercial finite-element-method solvers. Making use of the equivalence principle, it was demonstrated that by superimposing magnetic and electric surface currents at the boundary of an object, the scattered field from that object can be cancelled. Subsequently, these magnetic and electric surface currents were discretized into electric and magnetic dipoles that were physically implementable by straight and loop wire antennas. The authors presented numerical results in 2-D and 3-D simulation scenarios for electrically-small objects, of size 0.7 λ (where λ denotes the wavelength of the incident wave). For a metal cylinder in 3-D, a 20 dB reduction of the forward scattering was reported in simulations using this method.

In this work, we deploy a full-wave 2-D FDTD method with a highly accurate realization of the perfect total-field scattered-field (TFSF) interface [8,9] - specifically suited for the time-domain analysis of active invisibility of electrically-large objects. This particular TFSF implementation guarantees excellent isolation between the scattered- and total-field regions of the computational domain, right at the numerical noise level (−300 dB). Hence, and first, it is suitable for checking whether a considered cloak implementation is indeed perfect. Moreover, and quite crucially, it allows one to precisely evaluate the scattering levels of imperfect active electromagnetic cloaks - a subtle issue requiring, ideally, direct time-domain simulations, and which has not been studied in the past. To our knowledge, the TFSF implementation [8,9] has not been employed yet for precise (high-accuracy) simulations of the scattering from cloaking devices. In general,

Optics EXPRESS

due to the mismatch between the intended source implementation (analytic continuous-time solution) and the propagating wave in the descritized FDTD grid, non-physical reflections as large as 10% (−20 dB) of the incident plane wave can be observed in the scattered-field region when other implementations of the TFSF interface are deployed [10,11]. In our considered simulation scenarios, imperfect predetermined cloaks are also taken into consideration, canceling the scattered field by using arrays of current sources - with our developed FDTD code allowing one to directly simulate the current sources that are delayed in relation to the scattered field. Furthermore, it allows us to activate all current sources with a delay, or even simulate their activation with a given time of predetermination. Overall, our results allow for obtaining useful insights into the dependence of required scattering levels on active cloak imperfections.

2. Problem formulation

Let us consider an object in 2-D coordinate system which we are going to cloak, refer to Fig. 1(a). In our case, it is a cylinder made of the perfect electric conductor (PEC) of diameter 500 λ (where λ = 508.1 nm denotes the wavelength of the incident wave in the centre of the visible band 430–750 THz). We assume that appropriate electric and magnetic current sources are placed along the square around the PEC cylinder (i.e., along the cloak surface). The plane wave impinges on the cloak in the time t_1 and the wave then impinges on the PEC cylinder. Then, the scattered wave is propagated which impinges on the inner cloak surface in the time $t_2 > t_1$. Based on the surface equivalence theorem [6,12], one can cancel the scattered field with the use of current sources given by

$$\mathbf{J}_{cloak} = -\mathbf{n} \times \mathbf{H}_{scat} \tag{1}$$

$$\mathbf{M}_{cloak} = -\mathbf{E}_{scat} \times \mathbf{n} \tag{2}$$

where $\mathbf{J}_{cloak}$ and $\mathbf{M}_{cloak}$ denote respectively the density of electric and magnetic currents, $\mathbf{E}_{scat}$ and $\mathbf{H}_{scat}$ denote respectively the intensity of electric and magnetic scattered fields, and $\mathbf{n}$ denotes the unit vector directed outwards which is normal to the cloak surface (i.e., the closed curve in the 2-D case). However, this cloaking procedure requires the knowledge of the scattered field ($\mathbf{E}_{scat}$, $\mathbf{H}_{scat}$) at the cloak surface which might be difficult to determine in sufficiently short time. One can imagine [3] that the incident field ($\mathbf{E}_{inc}$, $\mathbf{H}_{inc}$) is known in the bottom-left corner of the cloak surface, hence, the scattered field can be computed in this point (i.e., locally) based on scattering characteristics of the volume to be cloaked (e.g., the PEC cylinder in the considered case). However, information about the incident wave is firstly known only in the point of the detection of the plane wave by the cloak (i.e., the bottom-left corner of the cloak surface). Hence, it has to propagate to the current sources along the cloak surface in order to calculate and then cancel the scattered field. The distance along the cloak surface is always longer than the distance which the incident wave propagates within the square cloak. Hence, a delay exists between the scattered field and the field generated by the current sources in order to cancel the scattered field.

Alternatively, one can imagine that the characteristics of the plane wave impinging on the object are known - hence, cloaking schemes have been proposed based on such an idea of 'predetermined' cloaking. In each current source along the cloak surface, it is possible to measure the total field ($\mathbf{E}_{total}$, $\mathbf{H}_{total}$) which is given by

$$\mathbf{E}_{total} = \mathbf{E}_{scat} + \mathbf{E}_{inc} \tag{3}$$

$$\mathbf{H}_{total} = \mathbf{H}_{scat} + \mathbf{H}_{inc}. \tag{4}$$

Then, in each current source, the scattered field can theoretically be determined by subtracting the measured total field and the predetermined incident field.

In both considered cases, the generation of currents along the cloak surface requires some time. Therefore, the reaction of the current sources to the incident plane wave is always delayed.

Optics EXPRESS

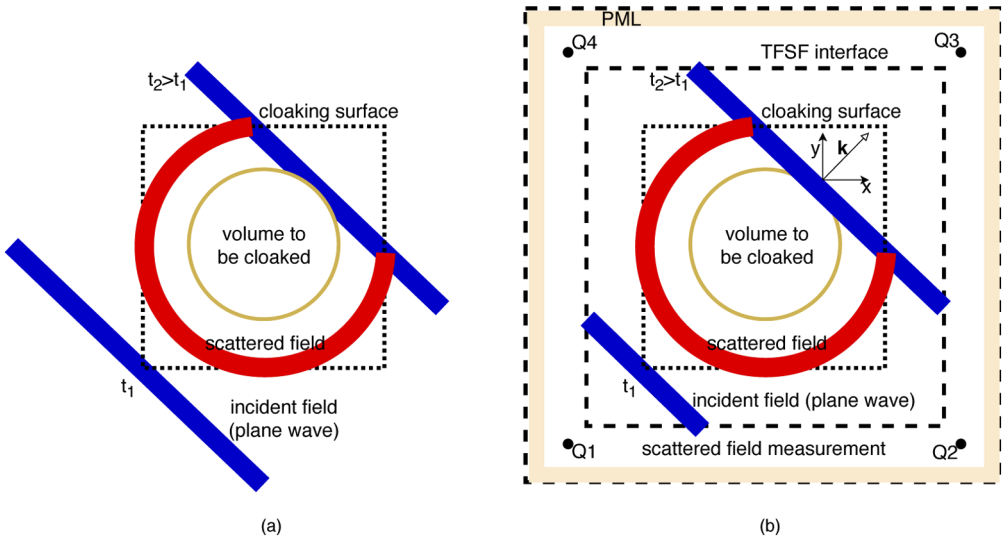

Fig. 1. Wave incident on the cloaked volume (PEC cylinder). (a) Cloaking scheme. (b) FDTD simulation scenario.

Unfortunately, to the best of the authors' knowledge, precise measurements of the influence of source delays on the scattering characteristics have not been presented yet. Furthermore, and crucially, the performance of the cloak for different predetermination times has not been presented yet. It is for such purposes that a high-accuracy FDTD/TFSF method can prove useful, as shown in some detail in the following.

We here note that the cloak geometry is not limited to square or rectangular shapes. That is, circular or even arbitrary shapes can be considered. However, due to the implementation of simulations with the use of a rectangular FDTD grid, the rectangular cloak is the simplest and preferable solution for our present investigations.

3. Simulation method

We start by outlining the characteristics and details of the 2-D TM_z FDTD method that we used (i.e., where the H_x, H_y, E_z field components are simulated). The correctness of the FDTD code has been corroborated by comparison with the corresponding solutions based on the FDTD-compatible discrete Green's function [13–15].

For 2-D TM_z simulations, complementary results can be obtained using the TE_z polarization. The TM_z and TE_z modes constitute the two possible ways that 2-D electromagnetic wave interaction problems can be set up for the case of zero partial derivatives in the z-direction [6]. Hence, our conclusions are not restricted to a given polarization of the plane wave, because one can decompose any 2-D simulation scenario into TM_z and TE_z FDTD simulations. Furthermore, this active cloaking scheme, based on the use of a Huygens surface, which is well established in wave physics and scattering theory, is indeed general, i.e., not restricted to a given polarization [12].

Let us consider the simulation setup presented in Fig. 1(b). The square geometry of the FDTD grid is assumed in our simulations (i.e., $\Delta x = \Delta y = 19.98$ nm). It stems from the fact that the numerical dispersion error of the non-square FDTD grid is larger than that of the corresponding square grid [16]. The size of the computational domain is set to $16\,000 \times 16\,000$ cells. The TM_z-polarized plane wave is generated at the TFSF interface around the cloak surface. For this purpose, multipoint auxiliary time-domain 1-D propagator [6,8,9] is implemented,

Optics EXPRESS

which guarantees the leakage error of the plane-wave injection at the numerical noise level. The angle ϕ between the wave vector $\mathbf{k}$ and the x-axis is set to 45° (parameters of multipoint auxiliary time-domain 1-D propagator are set to $m_x = 1$ and $m_y = 1$) if not stated otherwise. The distance between the TFSF interface and the domain boundary is set to 100 cells. The computational domain is terminated by the perfectly matched layers (PMLs) [6] implemented based on Berenger's approach [17]. The number of layers at each boundary being PMLs is set to 16. The distance between the cloak and the domain boundary is set to 200 cells. Hence, the side length of the square cloak is equal to $a = 15\,600\Delta x = 311.8\mu m$. It is assumed that the thickness of the cloak is equal to $\Delta r = \Delta x = \Delta y$. Hence, the current densities of numerical sources at the cloak in FDTD simulations are given by

$$\mathbf{J}_{cloak}^{FDTD} = \frac{\mathbf{J}_{cloak}}{\Delta r} = -\frac{\mathbf{n} \times \mathbf{H}_{scat}}{\Delta r} \tag{5}$$

$$\mathbf{M}_{cloak}^{FDTD} = \frac{\mathbf{M}_{scat}}{\Delta r} = -\frac{\mathbf{E}_{scat} \times \mathbf{n}}{\Delta r}. \tag{6}$$

The scattered field E_z is evaluated in three points Q1–Q3 within the scattered-field region (waveforms for Q2 and Q4 points are the same when $\phi = 45°$). Their coordinates are as follows: Q1(49,49), Q2(15 950, 49), Q3(15 950, 15 950). Hence, the backward and forward scattering characteristics correspond to the points Q1 and Q3, respectively. The point Q2 corresponds to 90° angle between the directions of incident and scattered waves. The Courant-Fridrich-Lewy factor being the ratio of the time-step size and the maximum stable time-step size [6] is set to 0.99. Hence, the time-step size in simulations is set to $\Delta t = 0.0467$ fsec. Each FDTD simulation is executed in 40 000 time steps. A wideband excitation is employed in the FDTD simulations to tackle bandwidth issues of the cloaks in the visible frequency range 430-750 THz. It is a Gaussian-modulated sinusoidal pulse presented in Fig. 2. For the sake of reference, the simulation of scattering from the PEC cylinder is executed without the cloak at first. It gives the reference level allowing one to evaluate how many times the field scattered by the PEC cylinder within the cloak is lower than that of the PEC cylinder without the cloak. Then, the cloak scattering is expressed in dB as $20 \log |E_z(f)/E_z^{ref}(f)|$, where $E_z^{ref}(f)$ denotes the frequency-domain field measured without the cloak in the considered point.

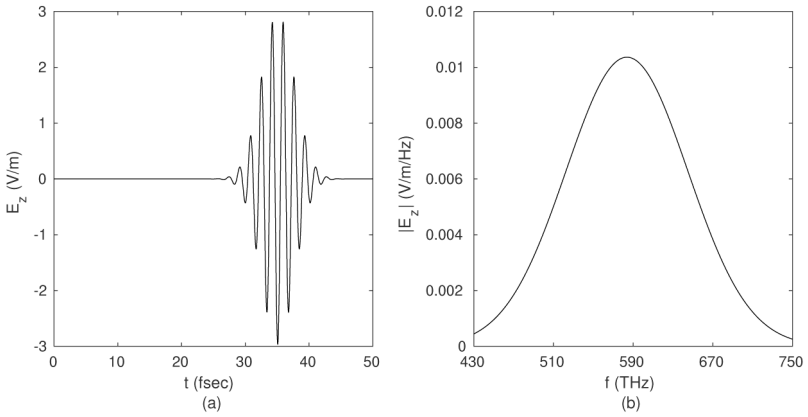

Fig. 2. Gaussian-modulated sinusoidal pulse recorded in the bottom-left corner of the cloak. (a) Time-domain waveform. (b) Amplitude spectrum.

Optics EXPRESS

4. Numerical results

In this section, on the basis of the afore-outlined methodology, we evaluate, both, in the frequency- and time-domain, the performance of an active cloak, including previously unexplored, yet crucial, issues, such as potential 'errors' (delays) in the activation of the active sources and/or the choice of the predetermination time.

4.1. Current sources synchronized with the scattered field

First, we examine the ideal case, where the current sources of the cloak generate an electromagnetic field perfectly canceling the scattered field; that is, the case where the cloak perfectly conceals over broad bands an electrically-large object.

To that end, in Fig. 3 the scattered field levels are presented in reference to the case without the cloak. As may be seen, the scattered field is indeed around the numerical noise level (−300 dB), confirming, both, the proper operation of the ideal cloak as well as the high-accuracy implementation of the predetermined cloaking in the discretized FDTD/TFSF space. It has been verified that the same scattering levels (i.e., numerical noise) are consistently observed for the cases where the incidence angle is set to $\phi = 68.2°$ ($m_x = 2$, $m_y = 5$), $\phi = 33.69°$ ($m_x = 3$, $m_y = 2$), and $\phi = 26.56°$ ($m_x = 2$, $m_y = 1$), thereby further confirming the correct implementation of the perfect TFSF interface.

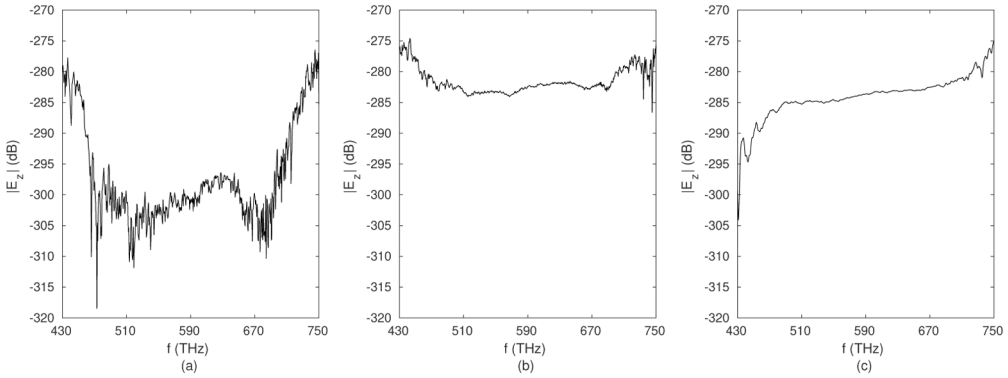

Fig. 3. Scattered field measured for the ideal cloak whose current sources are synchronized with scattered field and activated without any delay. (a) Q1. (b) Q2. (c) Q3.

Furthermore, it is found that the active cloak is sensitive to perturbations in the geometric positioning of the active sources. For instance, introduction of small gaps in the cloak by removing single electric and magnetic current sources may appreciably affect its performance. Specifically, as an example, 12 gaps spaced by a distance $1201\Delta x = 23.99$ μm, introduced in each side of the square cloak, increase the scattered field to levels around −39 dB (Q1), −41 dB (Q2) and −43 dB (Q3).

4.2. Delayed current sources

Next, we investigate the case where the current sources of the cloak generate an electromagnetic field imperfectly canceling the scattered field, i.e., the current waveforms are the same as in the previously considered case but now slightly delayed in time - indicating, for instance, for a real-life experiment, the potential occurrence of an error or inaccuracy in the switching on of the active sources. To that end, in Fig. 4 the scattered field levels at points Q1, Q2 and Q3 are presented across the entire visible band, relatively to the PEC cylinder without the cloak, and for current sources whose waveforms are only slightly delayed - in the example shown there, by a

Optics EXPRESS

single FDTD time step Δt. As may be seen, the scattered field increases immediately to levels around −33 dB (Q1), −14 dB (Q2) and −15 dB (Q3). This demonstrates that predetermined active cloaking is indeed appreciably sensitive to perturbations from the ideal scenario studied in the previous section. Interestingly, we may also see from Fig. 5 that even for a sufficiently long delay of (error in) the active-current waveforms, there still exists a frequency in the amplitude spectrum at which the scattering is suppressed. This result (physically) simply arises from the fact that, at that frequency point, the delay in the switching on of the active sources is equal to a period of the scattered field, thereby again allowing for the cancellation of the scattered field.

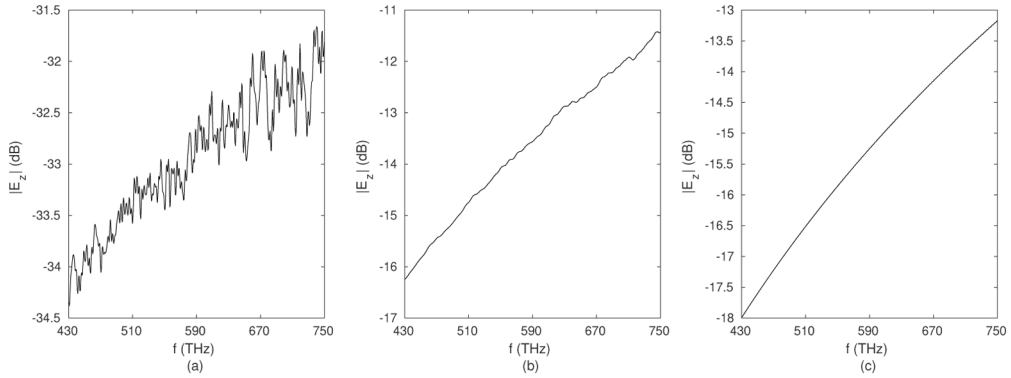

Fig. 4. Scattered field measured for the cloak whose current sources are delayed by time $t = 1\Delta t = 0.0467$ fsec. (a) Q1. (b) Q2. (c) Q3.

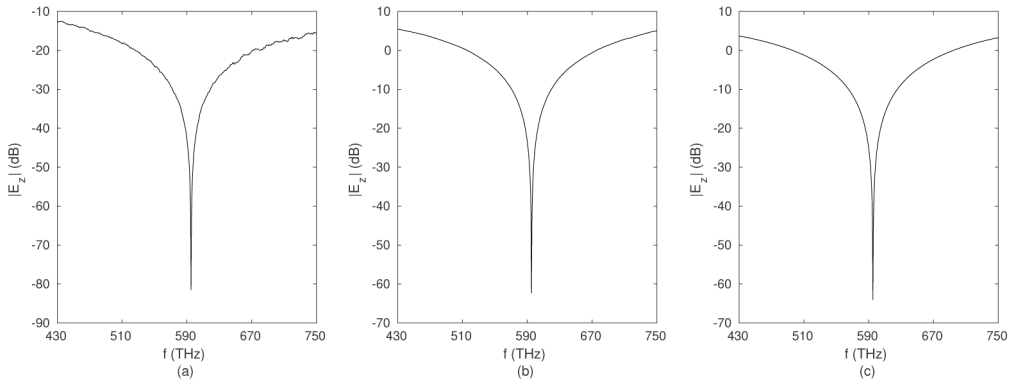

Fig. 5. Scattered field measured for the cloak whose current sources are delayed by time $t = 36\Delta t = 1.6801$ fsec. (a) Q1. (b) Q2. (c) Q3.

Figure 6 summarizes how fast, for three different frequencies (510 THz, 590 THz, and 670 THz), the performance of the active cloak deteriorates when the delay in the switching on of the sources is increased. One may see that the performance of the cloak deteriorates compared with the ideal (zero delay) case even for very small delays (errors), from which point onward the scattering does not change significantly with further delays. Furthermore, for longer delays, and for the Q2 and Q3 (high-symmetry) measurement points, the scattering actually becomes comparable to the one of the PEC cylinder without the cloak. However, the back-scattering (Q1 measurement point) is still maintained below 0 dB.

Optics EXPRESS

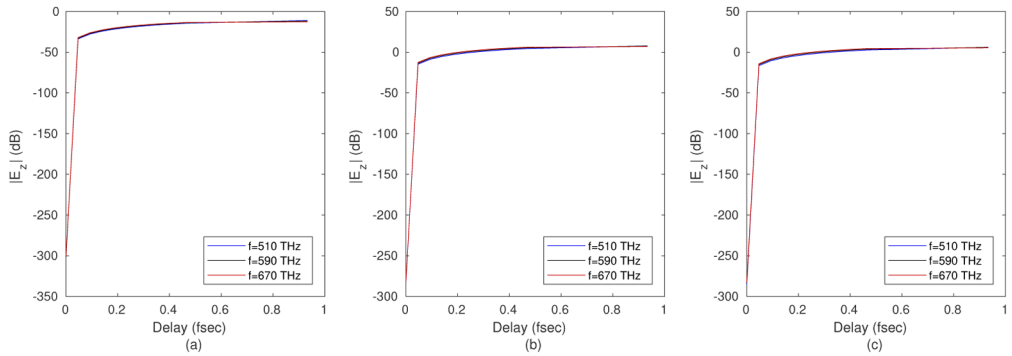

Fig. 6. Scattered field for frequencies 510, 590 670 THz measured for the cloak whose current sources are delayed. (a) Q1. (b) Q2. (c) Q3.

4.3. *Synchronized current sources activated by information transferred along cloak surfaces*

As already explained, the developed FDTD/TFSF methodology allows for simulations of active cloaks whose current sources are activated by information progressively being transferred along the cloak surface. To that end, we have assumed that the first contact of the incident wave with the cloak is in its lower-left corner. Then, information transfers concurrently along, both, the left-upper and bottom-right sides of the square cloak. Hence, the direction of information transfer is from bottom-left to upper-right corner of the cloak. In this section, in order to study the role of the predetermination time, we vary the effective 'speed of information' v_{inf} along the surface of the cloak. Values of v_{inf} larger than the speed of light in vacuum cannot, of course, occur owing to relativistic causality, thus they herein simply imply longer predetermination times - that is, how much ahead in time before the arrival of the incident wavefront on the surface of the cloak should an active source be switched on. Furthermore, for an even more experimentally-realistic scenario, we take that each current source (on the surface of the cloak) is activated only when the time measured from the first contact of the incident wave with the cloak is greater than the activation time given by

$$t_{active} = \frac{d}{v_{inf}} + t_{det} \tag{7}$$

where d denotes the distance to the current source along the cloak surface and t_{det} denotes the offset time resulting from the finite detection time of the signal in the lower-left corner of the cloak. For the presented results, the offset time resulting from the finite detection time was arbitrarily set to (a realistic value of) $t_{det} = 800\Delta t = 37.34$ fsec. This corresponds to the time moment after the passage of the maximum of the incident plane wave through the bottom-left corner of the cloak, see Fig. 2.

The results of our simulations are plotted as a function of the predetermination time t_{pred} for the upper-right corner of the cloak, that is, as mentioned above, the time delay between the arrival of the light wavefront propagating diagonally in the cloak and the information traveling along the cloak surface to the upper-right corner of the cloak

$$t_{pred} = \frac{\sqrt{2}a}{c} - \frac{2a}{v_{inf}} - t_{det}. \tag{8}$$

First, in Fig. 7, the scattered-field values are presented, in reference to the case without the cloak, for the ideal case where $t_{pred} = 0$ sec (this corresponds to an effective $v_{inf} = 1.45c$). As may be seen, the scattered field is indeed in this case around the numerical noise level, as it

Optics EXPRESS

should. Here, information travels the distance $2a$ (where a denotes the side length of the square cloak) whilst the plane wave propagates the distance $\sqrt{2}a$ within the cloak. Hence, for effective information speeds v_{inf} higher than around $\sqrt{2}c$ (notice the non-zero detection time t_{det}), i.e., for $t_{pred}>0$, it is indeed possible to observe broadband perfect cloaking of an electrically-large object.

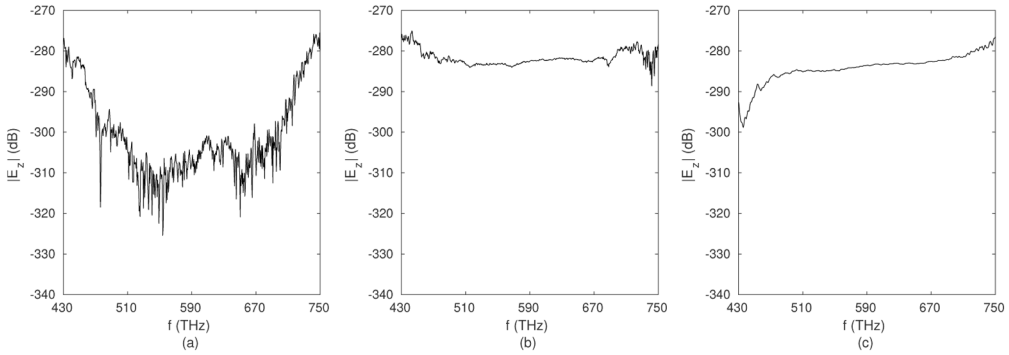

Fig. 7. Scattered field measured for the cloak whose current sources are activated by information transferred with $t_{pred} = 0$ sec along the cloak surface. (a) Q1. (b) Q2. (c) Q3.

In Fig. 8, the scattered field levels are presented, in reference to the case without the cloak, but now for the case where $t_{pred} = -26$ fsec (i.e., for a smaller effective information speed $v_{inf} = 1.425c$). As can be seen, the backward scattering (Q1) is still around the numerical noise level, however the scattering levels at the other measurement points deteriorate appreciably to around -130 dB (Q2) and -60 dB (Q3) - still, though, being overall, for those two points, a satisfactory cloaking performance. The forward scattering level (at point Q3) is even more sensitive to the decrease of the predetermination time, showing clearly that the 'really' challenging part in this cloaking scheme too (similarly to all other schemes) is to suppress the forward scattering, i.e., to prevent the 'shadow' effect of a cloak, thereby to allow for the incident wave to smoothly recombine in free space after it has traveled along the cloak's surface.

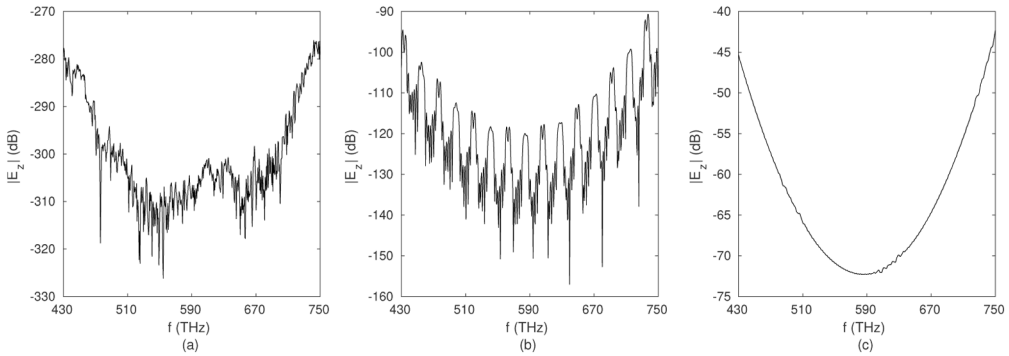

Fig. 8. Scattered field measured for the cloak whose current sources are activated by information transferred with $t_{pred} = -26$ fsec along the cloak surface. (a) Q1. (b) Q2. (c) Q3.

In Fig. 9, the scattered field levels are presented in reference to the case without the cloak but now for an even smaller effective information speed, corresponding to $t_{pred} = -39$ fsec ($v_{inf} = 1.4125c$). As may be seen, the backward scattering (Q1) is again around the numerical noise level, with the scattering at point Q2 being maintained at sufficiently good levels, but with the scattering level at the measurement point Q3 now having deteriorated significantly to around

Optics EXPRESS

0 dB (or above, indicating actually increased scattering owing to the active sources). In this case, the predetermination time is insufficient to activate the current sources in the upper-right corner of the cloak before the plane-wave's arrival at this point.

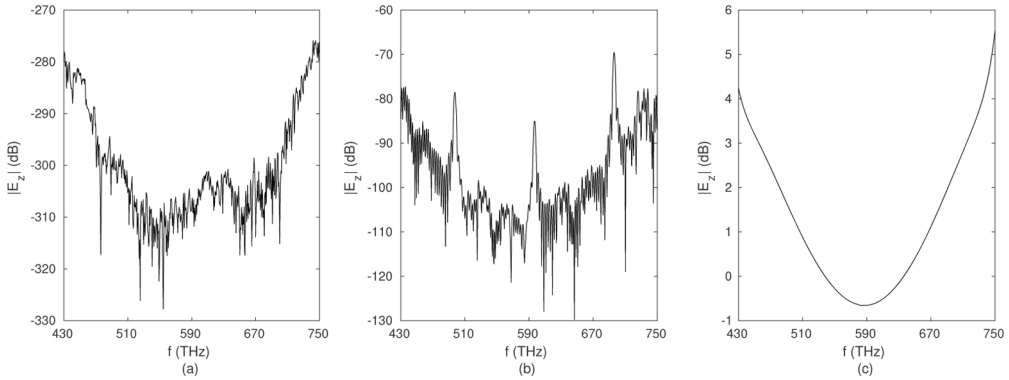

Fig. 9. Scattered field measured for the cloak whose current sources are activated by information transferred with $t_{pred} = -39$ fsec along the cloak surface. (a) Q1. (b) Q2. (c) Q3.

Finally, Fig. 10 summarizes how the performance of the cloak deteriorates, for three chosen frequencies (i.e., 510, 590, 670 THz), when the predetermination time takes on progressively higher negative values (corresponding to delay, i.e., to an effective error). As can be seen, the forward scattering (Q3) immediately approaches the level of 0 dB, and the curve characteristics remain flat when the predetermination time is set towards negative values. On the other hand, the backward scattering (Q1) is relatively insensitive to variations of the predetermination time because the current sources in the lower-left corner of the cloak are immediately activated, the incident wave then moves on inside the cloak, is back-scattered by the object, and upon returning (from the inside) to point Q1 the field value of the source at that point has become zero, trapping the field inside the cloak and preventing back-scattering to occur (see Fig. 1(a)). Overall, as may be seen, the improper (negative) values of the predetermination time result in a clear deterioration of the scattering performance of the cloak. Hence, one may conclude that the ideal active-cloaking performance with synchronized current sources activated by information transferred along its surface is quite sensitive to perturbations of (errors or inaccuracies in) the predetermination time. We also note that for the physically-allowed value of the effective information speed $v_{inf} = c$, the scattered field levels turn out to be around -135 dB (Q1), 0 dB (Q2), and 0 dB (Q3).

Optics EXPRESS

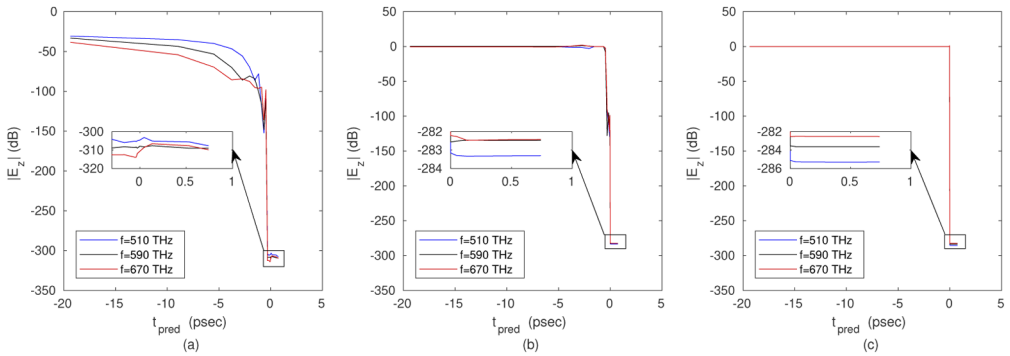

Fig. 10. Scattered field for frequencies 510, 590, 670 THz measured for the cloak whose current sources are activated by information transferred with varied speed. (a) Q1. (b) Q2. (c) Q3.

5. Conclusion

In summary, we have deployed a 2-D FDTD method combined with a perfect TFSF interface for evaluating active electromagnetic cloaks. The employed TFSF implementation guarantees the isolation between scattered- and total-field regions at the numerical noise level. As a result, it is suitable not only for directly demonstrating that an ideal cloak functions perfectly, but also for the evaluation of the scattering performance of imperfect (realistic) active cloaks. In the simulation scenarios we considered, the active cloaks worked by canceling the scattered field, using arrays of current sources.

Our approach allowed us to analyse the effect of current sources being delayed in relation to the scattered field. Furthermore, we also studied the activation of current sources due to information transfer along the cloak surface, for various predetermination times. We found that the performance of the active cloak is appreciably sensitive to the choice of those times, at least insofar as broadband operation is concerned. Our results, providing time- and frequency-domain insights into the response and characteristics of active cloaking, including realistic effects and device implementations, elucidate the strengths but also weaknesses of such schemes, and could help towards attaining true, broadband invisibility [18] of electrically-large objects.

Funding. Funding for Statutory Activities for the Faculty of Electronics, Telecommunications and Informatics, Gdansk University of Technology; Hellenic Foundation for Research and Innovation (1819).

Acknowledgement. The work of TPS was supported by Funding for Statutory Activities for the Faculty of Electronics, Telecommunications and Informatics, Gdansk University of Technology. The work of KB and KLT was supported by the General Secretariat for Research and Technology (GSRT) and the Hellenic Foundation for Research and Innovation (HFRI) under Grant 1819.

Disclosures. The authors declare no conflicts of interest.

References

1. J. David L. Lynch, *Introduction to RF Stealth* (Scitech Publishing, Raleigh, NC, 2004).
2. J. B. Pendry, D. Schurig, and D. R. Smith, "Controlling electromagnetic fields," Science **312**(5781), 1780–1782 (2006).
3. D. A. B. Miller, "On perfect cloaking," Opt. Express **14**(25), 12457–12466 (2006).
4. R. Fleury and A. Alù, "Cloaking and invisibility: a review (invited review)," Prog. Electromagn. Res. **147**, 171–202 (2014).
5. R. Fleury, F. Monticone, and A. Alù, "Invisibility and cloaking: Origins, present, and future perspectives," Phys. Rev. Appl. **4**(3), 037001 (2015).
6. A. Taflove and S. C. Hagness, *Computational electrodynamics: the finite-difference time-domain method* (Artech House, Norwood, 2005), 3rd ed.
7. M. Selvanayagam and G. V. Eleftheriades, "An active electromagnetic cloak using the equivalence principle," Antennas Wirel. Propag. Lett. **11**, 1226–1229 (2012).

Optics EXPRESS

8. T. Tan and M. Potter, "On the nature of numerical plane waves in FDTD," Antennas Wirel. Propag. Lett. **8**, 505–508 (2009).
9. T. Tan and M. Potter, "1-d multipoint auxiliary source propagator for the total-field/scattered-field FDTD formulation," Antennas Wirel. Propag. Lett. **6**, 144–148 (2007).
10. D. Merewether and R. Fisher, "An application of the equivalence principle to the finite-difference analysis of em fields inside complex cavities driven by large apertures," in *1982 Antennas and Propagation Society International Symposium*, vol. 20 (1982), pp. 495–498.
11. T. Tan and M. Potter, "Optimized analytic field propagator (o-afp) for plane wave injection in FDTD simulations," IEEE Trans. Antennas Propag. **58**(3), 824–831 (2010).
12. C. A. Balanis, *Antenna theory: analysis and design* (Wiley-Interscience, 2005).
13. J. Vazquez and C. G. Parini, "Discrete Green's function formulation of FDTD method for electromagnetic modelling," Electron. Lett. **35**(7), 554–555 (1999).
14. S. Jeng, "An analytical expression for 3-d dyadic FDTD-compatible Green's function in infinite free space via z-transform and partial difference operators," IEEE Trans. Antennas Propag. **59**(4), 1347–1355 (2011).
15. T. P. Stefański, "A new expression for the 3-d dyadic FDTD-compatible Green's function based on multidimensional z-transform," Antennas Wirel. Propag. Lett. **14**, 1002–1005 (2015).
16. A. Zhao, "Rigorous analysis of the influence of the aspect ratio of Yee's unit cell on the numerical dispersion property of the 2-d and 3-d FDTD methods," IEEE Trans. Antennas Propag. **52**(7), 1630–1637 (2004).
17. J.-P. Berenger, "A perfectly matched layer for the absorption of electromagnetic waves," J. Comput. Phys. **114**(2), 185–200 (1994).
18. K. L. Tsakmakidis, O. Reshef, E. Almpanis, G. P. Zouros, E. Mohammadi, D. Saadat, F. Sohrabi, N. Fahimi-Kashani, D. Etezadi, R. W. Boyd, and H. Altug, "Ultrabroadband 3d invisibility with fast-light cloaks," Nat. Commun. **10**(1), 4859 (2019).